

An Introduction to the Integrated Climate Model of the Center for Monsoon System Research and Its Simulated Influence of El Niño on East Asian–Western North Pacific Climate

HUANG Ping^{*1}, WANG Pengfei^{1,2}, HU Kaiming¹, HUANG Gang³,
ZHANG Zhihua⁴, LIU Yong¹, and YAN Bangliang¹

¹Center for Monsoon System Research, Institute of Atmospheric Physics, Chinese Academy of Science, Beijing 100190

²State Key Laboratory of Numerical Modeling for Atmospheric Sciences and Geophysical Fluid Dynamics,
Institute of Atmospheric Physics, Chinese Academy of Science, Beijing 100029

³Key Laboratory of Regional Climate-Environment Research for Temperate East Asia,
Institute of Atmospheric Physics, Chinese Academy of Science, Beijing 100029

⁴National Marine Environmental Forecasting Center, Beijing 100081

(Received 25 November 2013; revised 6 February 2014; accepted 31 March 2014)

ABSTRACT

This study introduces a new global climate model—the Integrated Climate Model (ICM)—developed for the seasonal prediction of East Asian–western North Pacific (EA–WNP) climate by the Center for Monsoon System Research at the Institute of Atmospheric Physics (CMSR, IAP), Chinese Academy of Sciences. ICM integrates ECHAM5 and NEMO2.3 as its atmospheric and oceanic components, respectively, using OASIS3 as the coupler. The simulation skill of ICM is evaluated here, including the simulated climatology, interannual variation, and the influence of El Niño as one of the most important factors on EA–WNP climate. ICM successfully reproduces the distribution of sea surface temperature (SST) and precipitation without climate shift, the seasonal cycle of equatorial Pacific SST, and the precipitation and circulation of East Asian summer monsoon. The most prominent biases of ICM are the excessive cold tongue and unrealistic westward phase propagation of equatorial Pacific SST. The main interannual variation of the tropical Pacific SST and EA–WNP climate—El Niño and the East Asia–Pacific Pattern—are also well simulated in ICM, with realistic spatial pattern and period. The simulated El Niño has significant impact on EA–WNP climate, as in other models. The assessment shows ICM should be a reliable model for the seasonal prediction of EA–WNP climate.

Key words: Integrated Climate Model (ICM), global climate model, El Niño, East Asian climate

Citation: Huang, P., P. F. Wang, K. M. Hu, G. Huang, Z. H. Zhang, Y. Liu, and B. L. Yan, 2014: An introduction to the Integrated Climate Model of the Center for Monsoon System Research and its simulated influence of El Niño on East Asian–western North Pacific climate. *Adv. Atmos. Sci.*, **31**(5), 1136–1146, doi: 10.1007/s00376-014-3233-1.

1. Introduction

Seasonal climate prediction is a challenging task and has important social and economic impacts (e.g., Huang, 2006; Huang et al., 2007). The seasonal prediction of East Asian–western North Pacific (EA–WNP) climate is increasingly dependent on atmosphere–ocean coupled general circulation models (AOGCM). However, state-of-the-art atmospheric general circulation models (AGCM) and AOGCMs possess marked systematic biases in reproducing the EA–WNP climate, including the climatological mei-yu rainband, circulation, and interannual variation (e.g., Brown et al., 2013;

Sperber et al., 2013; Song and Zhou, 2014).

To provide model results that support the seasonal prediction of the EA–WNP climate, a new AOGCM, the Integrated Climate Model (ICM), has been under ongoing development since 2008 at the Center for Monsoon System Research, Institute of Atmospheric Physics (CMSR/IAP), Chinese Academy of Sciences. This new model integrates the Hamburg Atmospheric General Circulation Model Version 5 (ECHAM5) (Roeckner et al., 2003) and the Nucleus for European Modeling of the Ocean Version 2.3 (NEMO 2.3) (Madec, 2008) using the Ocean Atmosphere Sea Ice Soil Version 3 (OASIS3) (Valcke, 2006) as the coupler. At its current stage, ICM has steadily integrated 1500 years without climate shift. In this study, we introduce the framework and configuration of the first version of ICM, and evaluate its simulation

* Corresponding authors: HUANG Ping
Email: huangping@mail.iap.ac.cn

skill through comparison with observations.

Because the primary goal of ICM is to improve the seasonal prediction of the EA–WNP climate, we evaluate in detail its simulation skill in this regard by examining its reproduction of the climatology and interannual variation of the regional EA–WNP climate and its connection with preceding El Niño events, one of the most important prediction factors. The main challenge in simulating the EA–WNP climate is a deficiency in the mei-yu rainband (Du et al., 2010; Song and Zhou, 2014). Models find it hard to reproduce the dominant interannual pattern of the EA–WNP summer climate, the East Asia–Pacific (EAP) pattern, or the Pacific–Japan (PJ) pattern, characterized by a meridional dipole pattern of a positive/negative rainfall anomaly associated with a cyclonic/anticyclonic circulation anomaly (Huang and Li, 1987; Nitta, 1987). As many studies suggest, the interannual pattern of the EA–WNP climate is dominated by the thermal status of the tropical Indo-Pacific Ocean associated with El Niño events (Huang and Wu, 1989; Zhang et al., 1996; Zhang et al., 1999; Wang et al., 2003; Huang et al., 2004; Huang and Huang, 2009; Xie et al., 2009; Huang and Huang, 2010). Thus, the present study also evaluates the regional climate of the tropical Pacific.

The anomalous western Pacific anticyclone is believed to be a bridge for the impact of El Niño events on EA–WNP climate anomalies. Wang et al. (2003) suggested a local air–sea positive feedback in which negative SST anomalies suppress local convection and trigger low-level anticyclone anomalies through emanating descending atmospheric Rossby waves, which in turn enhance negative SST anomalies on its southeast flank through evaporation under northeasterly trade winds. This local positive feedback mechanism can amplify the El Niño-triggered WNP anomalous anticyclone. Another mechanism, known as the tropical Indian Ocean (TIO) capacitor effect, emphasizes the bridging role

of the TIO (Xie et al., 2009). The warming of the TIO induced by El Niño events can persist through summer and emanate a warm Kelvin wave into the equatorial western Pacific, inducing northeasterly surface wind anomalies on the northern flank. The surface friction-induced subtropical divergence suppresses convection over the WNP and leads to an anomalous anticyclone in the lower troposphere. Therefore, the relationship between El Niño events and EA–WNP climate and the impact mechanism are further evaluated.

This paper is organized as follows. The model framework is described in section 2. The observational data and method are introduced in section 3. The climatology and interannual variation simulated in ICM are evaluated in sections 4 and 5, respectively. The influence of El Niño on the EA–WNP climate in the simulation is presented in section 6. And finally, a summary and discussion of the key findings of the study are presented in section 7.

2. Model

The first version of the ICM is a coupled atmosphere–ocean–sea ice model without flux adjustment. A schematic diagram of ICM is shown in Fig. 1. ICM consists of the ECHAM5 atmospheric model, the NEMO 2.3 oceanic and sea ice model, and the OASIS3 coupler. The framework of ICM is similar to the Kiel Climate Model (KCM) and SINTEX (Gualdi et al., 2003; Luo et al., 2005). ECHAM and NEMO were chosen as the atmospheric and oceanic components because they demonstrate high skill in simulating global general circulation and the EA–WNP regional climate, and existing coupled models already employing them show good stability and usability (Gualdi et al., 2003; Luo et al., 2005). OASIS3 is a universal coupler and has been used in many coupled models (Valcke, 2006).

ECHAM5, the fifth version of the European Centre for

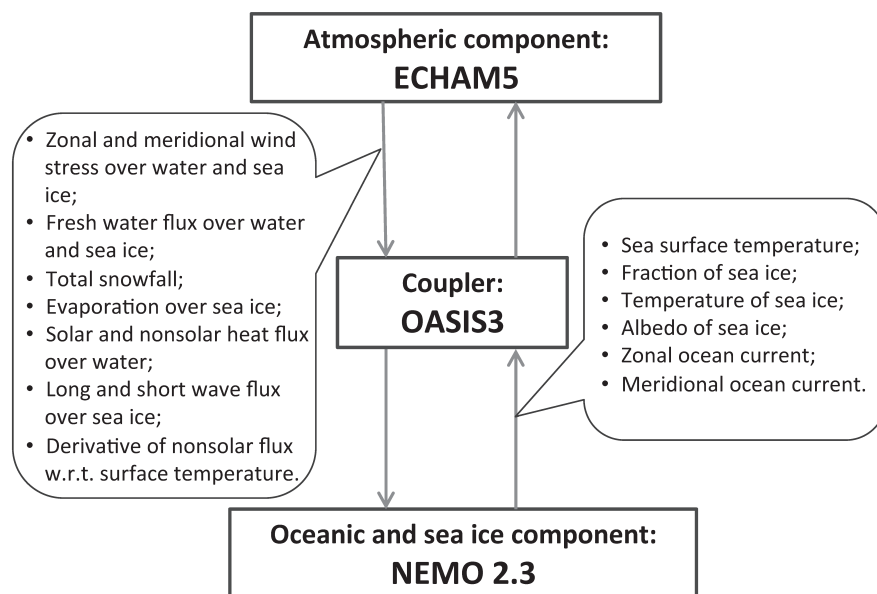


Fig. 1. Schematic diagram of ICM.

Medium-Range Weather Forecasts (ECMWF) model developed by the Max Planck Institute for Meteorology, is a spectral model with state-of-the-art physics (Roeckner et al., 2003, 2006). ECHAM5 shows strong performance in reproducing the climatological precipitation and interannual pattern of East Asian summer monsoon (e.g., Song and Zhou, 2014). The low-resolution version (T31; horizontal resolution: $3.75^\circ \times 3.75^\circ$; vertical resolution: 19 levels) of ECHAM5 is used in the first version of ICM. ECHAM5 has developed some higher-resolution versions, and thus the model resolution can be easily improved in future versions of ICM. More details about ECHAM5 can be found in Roeckner et al. (2003).

NEMO 2.3 includes the Ocean Parallelise Version 9 (OPA9) ocean general circulation model (OGCM), developed by the Institut Pierre-Simon Laplace (IPSL) (Madec, 2008), and the Louvain-la-Neuve Ice Model Version 2 (LIM2) sea ice model, developed by Louvaine-la-Neuve (Fichefet and Maqueda, 1997). The ocean component, OPA9, is a finite difference OGCM and an Arakawa C-grid is used to solve the primitive equations. OPA9 uses a global orthogonal curvilinear ocean mesh to move the mesh poles to the Asian and North American continents for avoiding the singularity point problem in the computational domain. The horizontal grid of NEMO uses an ORCA2 grid with a horizontal grid resolution of $182 (\text{lon}) \times 149 (\text{lat})$ (around 2° at high latitudes and an enhanced meridional resolution of 0.5° close to the equator) and 31 vertical levels to a depth of 5250.23 m with 10 levels in the top 100 m. NEMO calculates vertical eddy diffusivity and viscosity coefficients using a 1.5 turbulent closure scheme, allowing explicit mixed layer formulation and minimum diffusion in the thermocline. More details about NEMO can be found in Madec (2008).

The OASIS3 coupler is used for communication between ECHAM5 and NEMO in ICM (Valcke, 2006). Seventeen variables including wind stress, surface heat flux and freshwater flux are transferred from ECHAM5 to NEMO, while six variables including sea surface temperature, fraction, temperature and albedo of sea ice, and surface ocean current

speed are transferred from NEMO to ECHAM5 (Fig. 1). The vector of wind stress is passed to NEMO for two grids, the u grid and v grid of ORCA2. Bilinear interpolation is used to re-grid the variables exchanged between NEMO and ECHAM5 grids during the transfer process in OASIS3. The vector variables are rotated during transfer, because the grid directions are different in NEMO and ECHAM5. The time steps of the atmospheric and oceanic models are both 2400 seconds. The coupling frequency is once per 4 hours (six time steps).

3. Data and method

The datasets used for evaluating the model simulation include SST from the Hadley Center (HadISST) (Rayner et al., 2003), large-scale atmospheric circulation from the National Centers for Environmental Prediction/National Center for Atmospheric Research (NCEP/NCAR) reanalysis (Kalnay et al., 1996), and precipitation from the Global Precipitation Climatology Project (GPCP) (Adler et al., 2003). The model SST and atmospheric variables are re-gridded to the grid of HadISST ($1^\circ \times 1^\circ$) and the grid of NCEP/NCAR reanalysis data ($2.5^\circ \times 2.5^\circ$), respectively. A section of 100 years in the model is randomly selected after a 1000-year steady simulation to be compared with the observations for the period from 1981 to 2010. The climatologies in the model and observations are defined as the long-term mean of the aforementioned 100 years and 30 years, respectively. The interannual anomalies are defined as the deviation from the climatology. All analyses are based on these time periods unless otherwise specified.

4. Climatology

Figure 2 shows the time series of global mean SST in the 1500-year free-coupled integration of ICM. The global mean SST is stable at $18.36^\circ\text{C} \pm 0.04^\circ\text{C}$ after the first year, indicating no remarkable climate drift in the coupled integration.

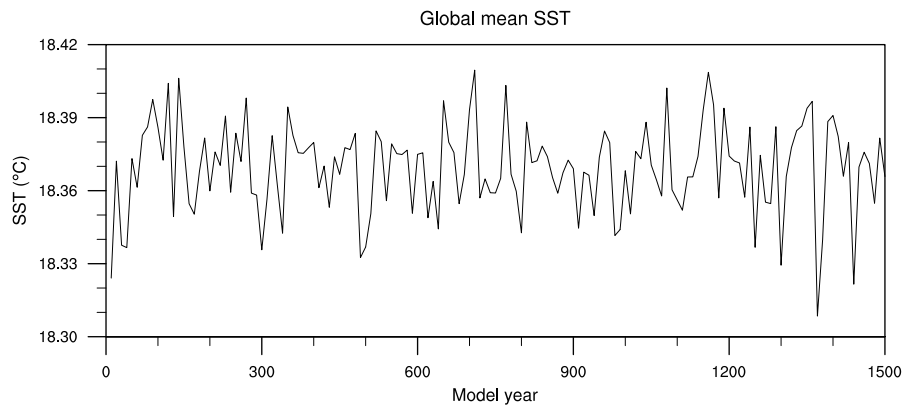


Fig. 2. Time series of the global mean SST ($^\circ\text{C}$) for the period from model year 1 to 1500. The time points are shown at an interval of 10 years and each time point represents the mean of 10 years around this point.

The simulated spatial pattern of SST for the seasonal mean [June–August (JJA) and December–February (DJF)] is compared with HadISST observations (Fig. 3). The common bias of SST is around 1°C–2°C (Figs. 3e and f). The main bias in the tropics is an excessive cold tongue that extends too far west into the western Pacific, which is also a common bias in KCM, SINTEX, and other AOGCMs (Gualdi et al., 2003; Luo et al., 2005; Park et al., 2009; Zheng et al., 2012; Li and Xie, 2014). The simulated excessive cold tongue could be attributed to the too strong zonal heat advection induced by the too strong trade winds (Zheng et al., 2012). We also find a warm bias along the east coast of South America, North America, and Africa, as in many CGCMs (Davey et al., 2002; Park et al., 2009), possibly due to the defective description of coastal upwelling. The simulated SST in ICM has no great bias in the midlatitudes of the North Atlantic, which is also obtained in KCM with the same model framework (Park et al., 2009).

The distribution of simulated precipitation is compared with GPCP observations in Fig. 4. The simulated tropical precipitation reproduces the main characteristics without the

apparent double-ITCZ problem common in many AOGCMs (e.g., Mechoso et al., 1995; Ma et al., 1996; Li and Xie, 2014). One conspicuous bias is insufficient precipitation over the equatorial central Pacific, with overestimated precipitation over the flanks (around 10°), which must be associated with the excessive cold tongue (Li and Xie, 2014). The simulated precipitation reproduces a quite realistic subtropical rainband over East Asia and North America (Fig. 4).

The seasonal cycle of equatorial Pacific SST has great importance to the development of El Niño in both observations and models (e.g., Wang and Picaut, 2004; Guilyardi, 2006), but its simulation exhibits systematic errors in many models (Latif et al., 2001; Guilyardi, 2006). In Fig. 5, the simulated seasonal cycle—deviation from the annual mean—of equatorial Pacific SST agrees well with the observations, including the realistic strength, the westward phase propagation, and the annual (semi-annual) cycle over the eastern (western) Pacific. The two main discrepancies between the model and observations are the discontinuous westward phase propagation in the model and the simulated boundary of the annual and semi-annual cycle being at around 180° east of the ob-

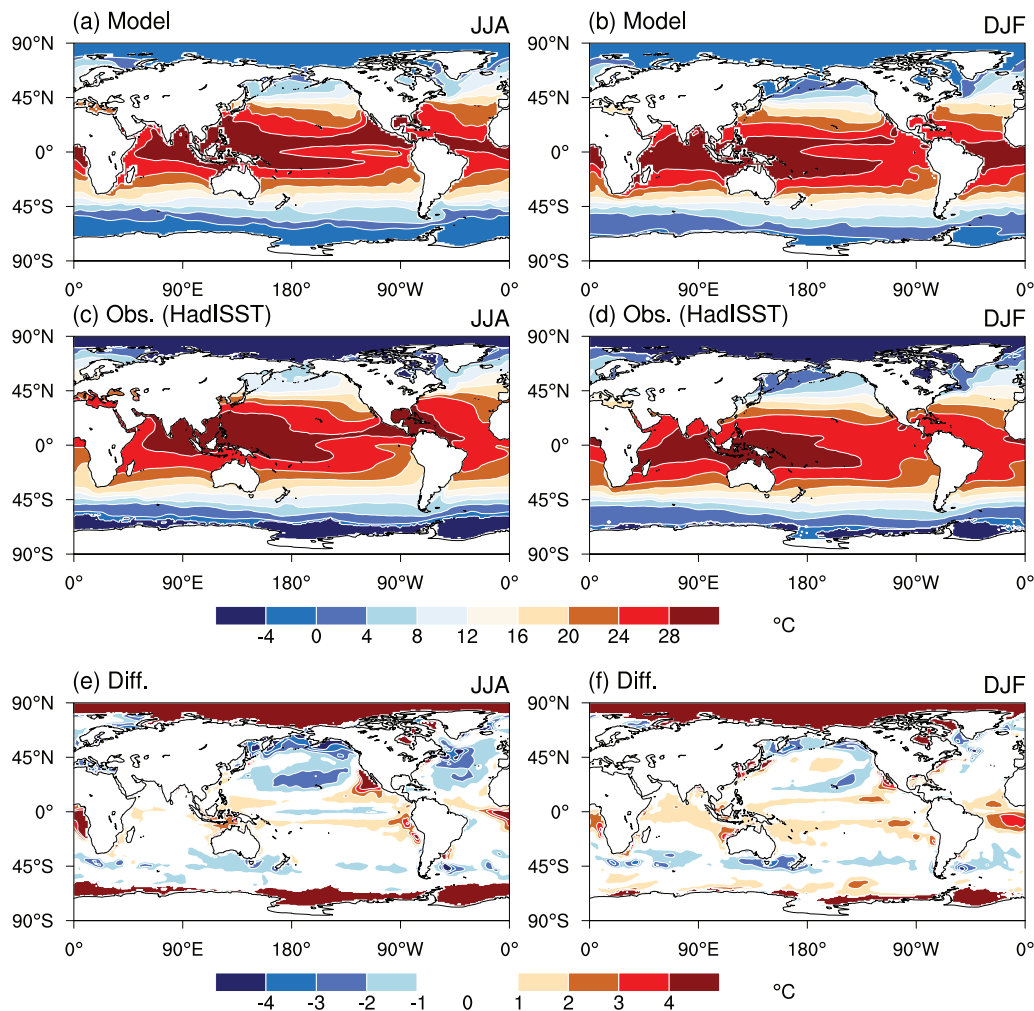


Fig. 3. Distribution of the (a, b) modeled and (c, d) observed SST (°C) in JJA and DJF for the periods as defined in section 2, and (e, f) their differences.

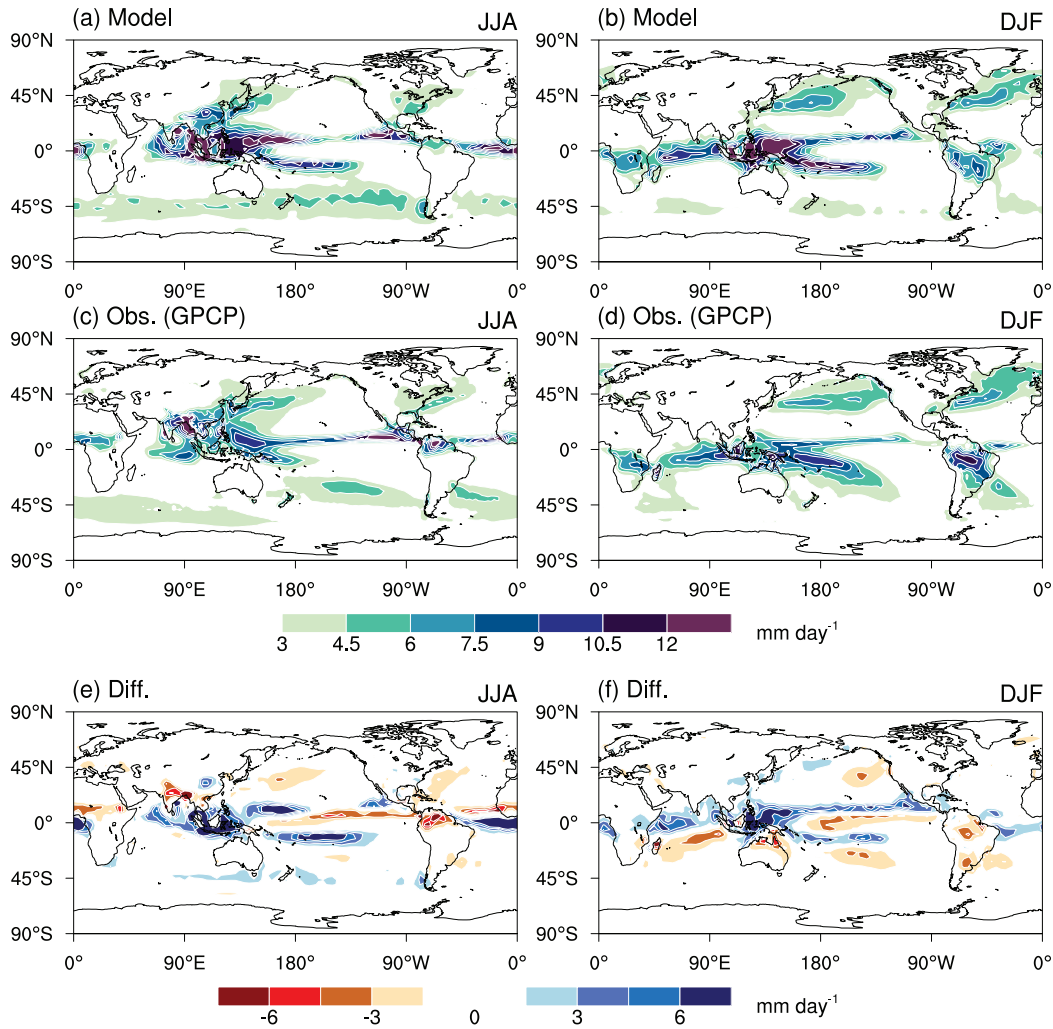


Fig. 4. The same as Fig. 3, but for precipitation.

served boundary at around 160°E . Some white bands in Fig. 5a representing missing values are induced by the model's low horizontal resolution. Because of the low model resolution, several oceanic grids near islands, with real values in the observed high-resolution HadISST (Fig. 5b), are inaccurately regarded as land and assigned to missing values.

For the EA–WNP climate, the simulation of the monsoon system, including precipitation and circulation, is the most important indicator of a model's skill over this region (Du et al., 2010; Sperber et al., 2013; Song and Zhou, 2014). The simulated EA–WNP climate by ICM is shown in Fig. 6a. The summer (JJA mean) mei-yu rainband is well simulated, with a realistic pattern and strength. However, the WNP anticyclone is overestimated, which induces the oceanic part of the mei-yu rainband to be located north of the observations.

5. Interannual variation

The dominant interannual variation of the EA–WNP climate is the EAP pattern (Huang and Li, 1987) or the PJ pattern (Nitta, 1987; Kosaka and Nakamura, 2006), which is closely associated with the interannual anomaly of the EA–

WNP climate (e.g., Huang et al., 2007). As in Kosaka et al. (2013), the EAP pattern is calculated by first performing empirical orthogonal function (EOF) analysis on the summer-mean (JJA) 850-hPa vorticity anomaly (0° – 60°N and 100° – 160°E), and then the principal component of the EOF's first mode is regressed on the precipitation and 850-hPa wind anomaly (the anomaly is based on the periods described in section 2 for the model and observations). The meridional structure of the EAP pattern, the meridional positive/negative rainfall pattern associated with the cyclonic/anticyclonic circulation pattern, is well described in the model compared to the observations (Figs. 6c and d). The magnitude of simulated precipitation is approximately the same as that in the observation. This performance of ICM is quite favorable with respect to most models in CMIP3 and CMIP5 (Song and Zhou, 2014). However, the magnitude of simulated wind shows great discrepancy with the observation. The observed wind anomalies associated with the EAP are stronger at lower latitudes than at higher latitudes, whereas the simulated wind anomalies are stronger at higher latitudes (Figs. 6c and d).

The dominant interannual variation of global climate is the variation of tropical Pacific SST associated with ENSO

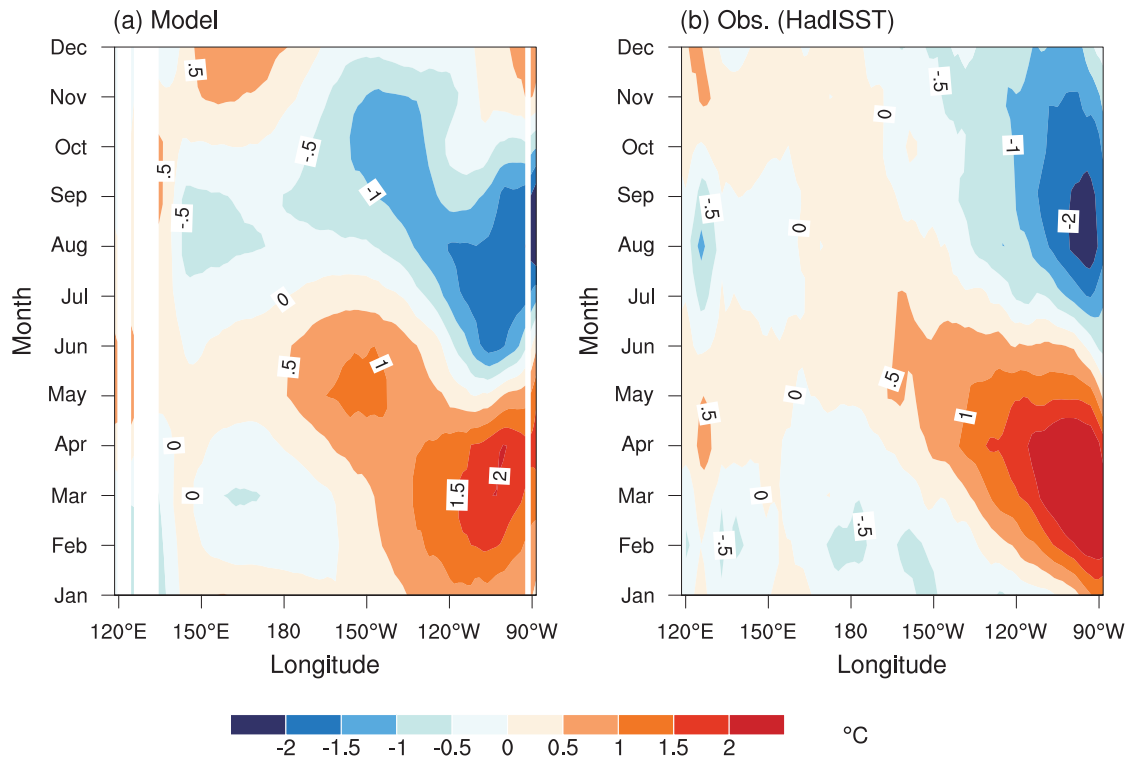


Fig. 5. (a) Modeled and (b) observed seasonal cycle of SST deviation from the annual mean ($^{\circ}\text{C}$) over the equatorial Pacific.

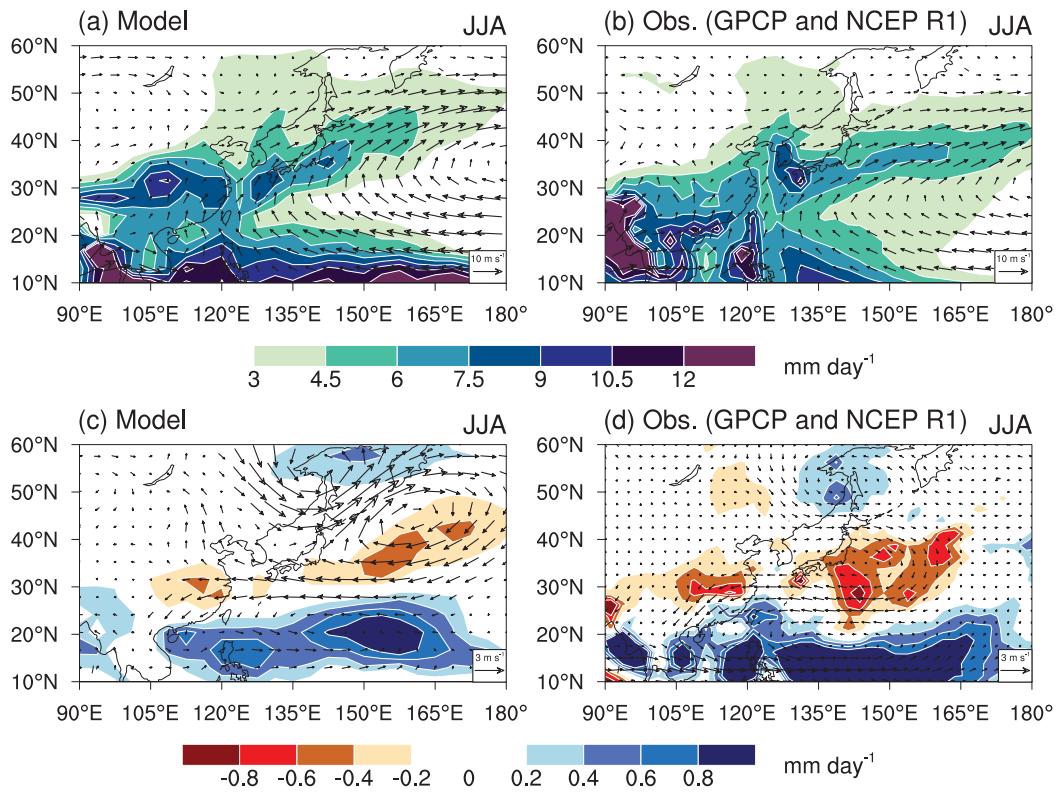


Fig. 6. (a) Modeled and (b) observed climatological precipitation and 850-hPa wind over the EA-WNP in summertime (JJA), and the (c) modeled and (d) observed East Asia-Pacific (EAP) pattern in JJA.

(e.g., Wang and Picaut, 2004; Deser et al., 2010). Figure 7 shows the simulated interannual variance, variance-period spectra, and regression onto the Niño3 index of tropical Pacific SST. The strength and pattern of the simulated interannual variance of the tropical Pacific SST anomaly (SSTA) are consistent with observations (Figs. 7a and b). The two discrepancies, i.e., the simulated interannual variance extending farther west than the observations and the variance along the east coast of South America being weak, are similar to what

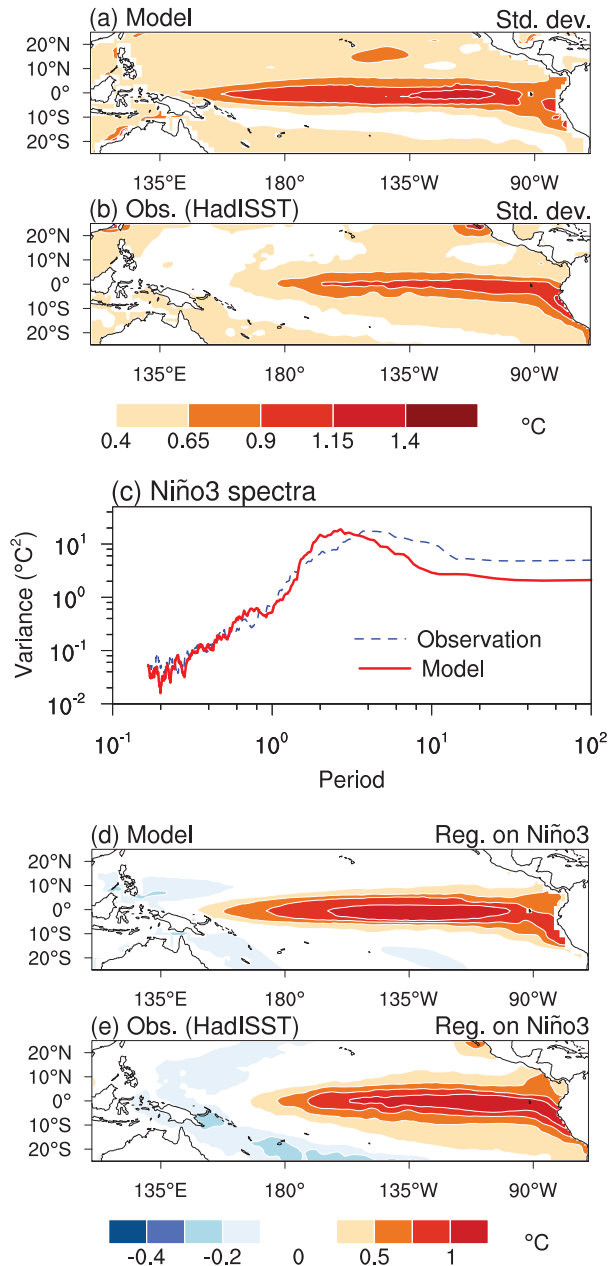


Fig. 7. Standard deviation of interannual variability of tropical Pacific SST in (a) the model and (b) observations. (c) Variance-period spectra of Niño3 index in the model and observations. Regression of tropical Pacific SSTA onto the Niño3 index in (d) the model and (e) observations. The results of the model and observations are based on the model-year period of 1001–1100 and 1911–2010, respectively.

has been found in KCM (Park et al., 2009), which could be associated with the biases of climatology. Niño3 index, defined as the regional-mean SSTA for 5°S–5°N and 90°–150°W, is used to represent the temporal variation of El Niño events. The spectrum of Niño3 index in the model is similar to the observations in terms of variance and period (Fig. 7c). The dominant variation is at a period of 3 years in the model—less than that in the observations (around 4 years). The simulated Niño3 index has much weaker variability at lower frequency than in the observation, indicating the current version of ICM has low skill in presenting the interdecadal variation. The regression of tropical Pacific SST onto the Niño3 index represents the spatial pattern of SSTA in El Niño events (Figs. 7d and e). The simulated SSTA pattern captures the well-known El Niño pattern (Rasmusson and Carpenter, 1982). The bias in the SSTA pattern occurs over similar places to the bias in the SSTA standard deviation (Figs. 7a and b). Compared with the observation, the simulated warm tongue in El Niño3 events extends too far west, which leads to a weak cooling in the western Pacific. The reasonable variance and period of Niño3 index with the spatial pattern of tropical Pacific SSTA shows ICM can reproduce El Niño events reasonably well.

6. Influence of El Niño on East Asian–western North Pacific climate

We use DJF-mean Niño3 index to denote the interannual variation of ENSO. Figures 8a and b show the model and observed JJA EA–WNP rainfall and 850-hPa wind anomalies regressed on normalized DJF(0) Niño3 index. DJF(0) represents the DJF mean of the last year. In the observations, anticyclone anomalies occur over the WNP and cyclone anomalies in the midlatitudes extending from northeast China to Japan. Associated with the dipole wind anomalies, the rainfall anomalies over the EA–WNP also display a dipole structure, with more (less) rainfall in the north (south) flank of the WNP anomalous anticyclone. The results show that the WNP summer monsoon is suppressed while the mei-yu front is enhanced, consistent with previous observational analyses (Zhang et al., 1996; Zhang et al., 1999; Wang et al., 2003). The dipole wind and rainfall anomalies over the EA–WNP in the El Niño decaying summer can basically be obtained in the model as they are in the observations (Figs. 8a and b), although the simulated cyclone anomalies in the midlatitudes are weaker than in the observations. Both in the model and the observations, the enhanced southwest winds in the west flank of the WNP anomalous anticyclone can induce a positive rainfall anomaly in China in that part of the anticyclone. Compared to observations, the model dipole rainfall and wind anomalies are more significant in the east relative to the west, which could be attributed to the overestimated equatorial rainfall anomalies around 160°E in the model. The bias of circulation and rainfall is possibly related to the unrealistic simulation of El Niño3-related SST anomalies. Figures 8c and d show the correlation map of JJA SST with

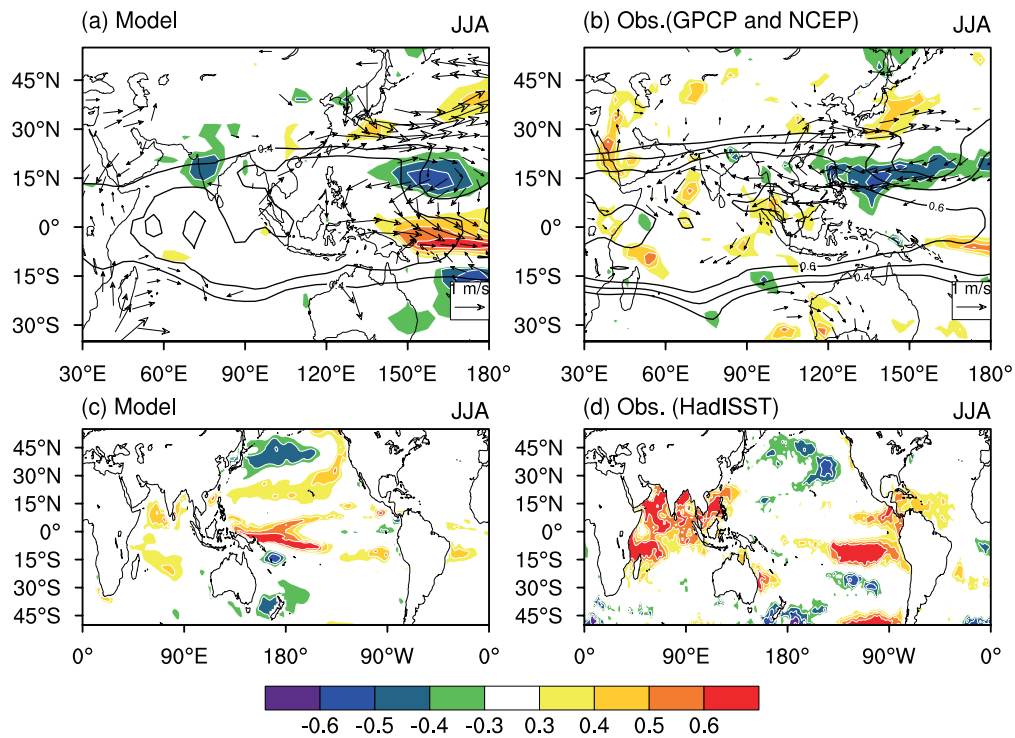


Fig. 8. Correlation of JJA precipitation (colors) and 200-hPa potential height (contours) with DJF(0) Niño3 index, and regression of 850-hPa wind (vectors) onto DJF(0) Niño3 index in the model and observations (upper panels). Correlation of JJA SSTA with DJF(0) Niño3 index in the model and observations (lower panels).

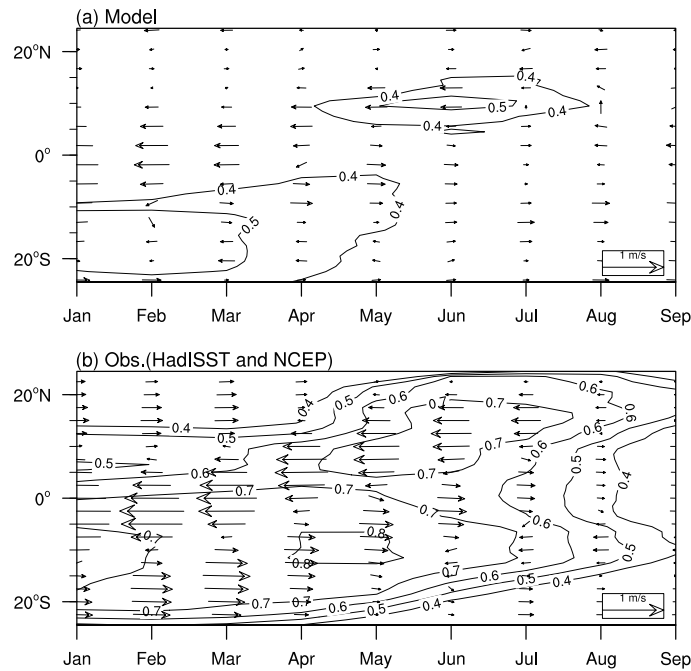


Fig. 9. (a) Modeled and (b) observed correlation (contours) between zonal-mean tropical Indian Ocean SST (40°–100°E) and the DJF Niño3 index, and regression (vectors) of zonal-mean 850-hPa wind upon the Niño3 index, as a function of calendar month and latitude.

DJF(0) Niño3 index in the model and observations. We can see that the model is able to reproduce realistic SST anoma-

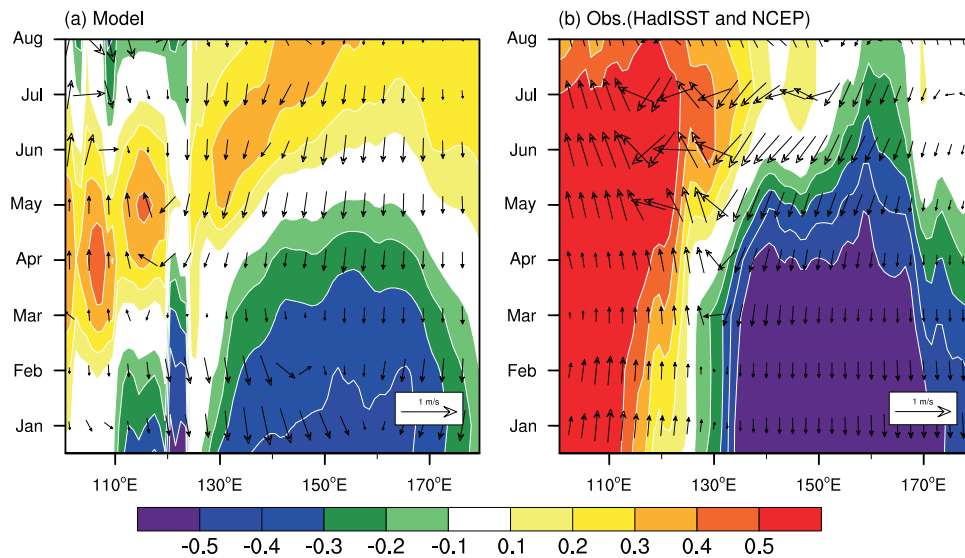


Fig. 10. (a) Modeled and observed regression of meridional-mean (5° – 20° N) 850-hPa winds and correlation coefficients of meridional-mean SST with DJF(0) Niño3 index, as a function of calendar month and longitude.

lies in most regions except the equatorial western Pacific, where there is an unrealistically strong SST warming center, which could lead to the overestimated rainfall and eastward shift of the northwest Pacific anomalous anticyclone. The unrealistic SST anomalies in turn are possibly related to the overly westward extension of the El Niño warm tongue in the model.

Regarding the impact mechanism of El Niño on EA–WNP climate in the model, the TIO capacitor effect is first examined. Figure 8 shows the correlation of JJA 200-hPa potential height with the DJF(0) Niño3 index (contours). In the observations, the 200-hPa height anomalies display a Matsuno–Gill pattern over the TIO and western Pacific, with a Kelvin wave trough in the equatorial western Pacific and two Rossby tails in the western Indian Ocean (Xie et al., 2009). The model can reproduce the Kelvin wave trough over the equatorial western Pacific. Over the TIO, although the two Rossby tails are not obvious, the 200-hPa heights are above normal. The results suggest that the model can reproduce the ENSO-related circulation anomalies over the TIO and western Pacific. Furthermore, the evolution of SST and 850-hPa wind anomalies in the El Niño decaying year are examined in Fig. 9. The observed maximum SST anomalies persist from January to May in the south TIO and extend north in JJA. The south TIO SSTA is induced by the El Niño-related downwelling oceanic Rossby wave and atmospheric bridge effect. In MAM, there are equatorial asymmetric wind anomalies over the TIO—westerly (easterly) wind in the south (north) TIO—which favor north TIO warming by reducing the climatological westerly winds. The easterly anomaly can persist to JJA and maintain the TIO warming to summer. In the simulation, the ENSO-related SST and wind anomalies pattern is the same as in the observations, including the persistent SST warming, the equatorial antisymmetric wind anomalies

in MAM, and the easterly anomalies in JJA. These results indicate the model possesses high skill in reproducing the TIO capacitor effect.

The local air–sea interaction mechanism is examined in Fig. 10. Figures 10a and b compare the correlation (regression) of zonal averages of SST (850-hPa wind anomalies) with (onto) DJF(0) Niño3 index between the observations and model. The observed El Niño-related wind anomalies are characterized by an anticyclonic shear over the WNP from January to July, associated with positive (negative) SST anomalies under the west (east) flank of the anticyclone. In the model, the anticyclonic shear wind anomalies and east–west SSTA dipole only persist until May, which is shorter than in the observations. In JJA, such air–sea positive feedback does not exist, which is consistent with most coupled models in CMIP5 (Hu et al. 2014). The possible reasons for weak air–sea positive feedback in coupled models needs further investigation.

Overall, the model demonstrates good skill in reproducing the anomalies of EA–WNP summer climate during the decaying years of El Niño events. The simulated impact mechanism of El Niño on the EA–WNP summer climate is dominated by the Indian Ocean capacitor effect, as in observations (Xie et al., 2009).

7. Summary and discussion

The present study introduces a new atmosphere–ocean general coupled model, ICM, developed by CMSR/IAP for the seasonal prediction of the EA–WNP climate. ICM uses ECHAM5 and NEMO 2.3 as the atmospheric and oceanic components, respectively, coupled by OASIS3. The first version of ICM is a low-resolution version, with a horizontal resolution of $3.75^{\circ} \times 3.75^{\circ}$ for the atmospheric component and

around 2° for the oceanic component. The model has steadily integrated up to 1500 years without climate shift.

The climatology, seasonal cycle and interannual variation of the simulation are evaluated. The model can reproduce a realistic distribution of seasonal SST, with a 1°C–2°C bias relative to observations in the tropics. The seasonal cycle of equatorial Pacific SST—a common challenge of AOGCMs—is also reasonably simulated, although the westward phase propagation of tropical SST is not accurately described. The main biases of ICM are the excessive cold tongue associated with the deficient precipitation over the central Pacific, as in many other models. The dominant interannual pattern of the tropical Pacific, El Niño events, is reproduced with a realistic spatial pattern, variance and period, whereas the interdecadal variation of tropical Pacific SST is underestimated in the model.

The mei-yu rainband of East Asian summer monsoon is another challenge for AOGCMs. ICM successfully reproduces the main characteristics of the mei-yu rainband with realistic pattern and strength. The dominant interannual pattern of East Asian summer monsoon, the EAP (or PJ) pattern, including its meridional structure and strength, can also be simulated by ICM. The simulated meridional dipole of the EAP pattern has a quite realistic positive/negative distribution of precipitation anomaly, whereas the simulated cyclonic/anticyclonic circulation anomaly associated with the EAP pattern is stronger at higher latitudes than at lower latitudes, which is different from the observations.

The observed dipole wind and rainfall anomalies, the anticyclone (cyclone) anomalies over the low-latitude (midlatitude) WNP, during the decaying period of El Niño events, can be well reproduced in the model. Even at the west flank of the dipole anomalies, the simulated rainfall anomalies in China are also highly consistent with observations. This result shows the model possesses good skill in simulating the influence of El Niño on the EA–WNP climate. The evolution of the two impact mechanisms—the local air–sea interaction effect and the TIO capacitor effect—shows that the model can reproduce the process of the TIO capacitor effect but not the local air–sea interaction effect. In the model, the TIO warming induced by the TIO antisymmetric wind and atmospheric teleconnection associated with El Niño can persist to summer and induce the WNP anticyclonic anomalies by emanating a warm Kelvin wave into the equatorial western Pacific, as in observations (Xie et al., 2009); whereas, the simulated anticyclonic shear wind anomalies and east–west SSTA dipole cannot persist to JJA, as suggested by the local air–sea interaction mechanism (Wang et al., 2003). This result, as in most CMIP5 models, indicates that the TIO capacitor effect is the dominant mechanism in the simulated influence of El Niño on EA–WNP climate.

The evaluations show ICM can successfully simulate the main characteristics of interannual variation of tropical Pacific SST and the EA–WNP summer monsoon, and reproduce their connection mechanism. They indicate the current version of ICM possesses good simulation skill and is a reliable AOGSM for the seasonal prediction of EA–WNP climate.

Although the current version of ICM successfully reproduces a lot of important aspects associated with the EA–WNP climate anomaly, some crucial biases still exist. The most important problems that should be addressed are the excessive cold tongue and the unrealistic westward phase propagation of equatorial Pacific SST, which could lead to unrealistic development of El Niño events and thus decrease the skill of seasonal climate prediction. As suggested by previous studies, the excessive cold tongue is coupled with the deficient precipitation and surface easterly wind bias, and arises from the air–sea coupled Bjerknes feedback (Zheng et al., 2012; Li and Xie, 2014). A similar bias in SINTEX, whose framework is the same as ICM, was reduced by including the westward ocean current to calculate the easterly wind stress (Luo et al., 2005). Without this process, the surface easterly wind stress and cold tongue will be significantly overestimated due to the Bjerknes feedback. Therefore, using more realistic air–sea coupling physics should be our next step to improve the model.

Although the primary goal in developing ICM is to apply it to the seasonal prediction of EA–WNP climate, our evaluation of its skill in this regard also shows that it can be used in broader climate studies, such as the impact mechanism of tropical SSTA on EA–WNP climate, the interannual variation of EA–WNP climate, and EA–WNP climate change under global warming.

Acknowledgements. This study was supported by the National Basic Research Program of China (Grant Nos. 2012CB955604 and 2014CB953903) and the National Natural Sciences Foundation of China (Grant No. 41375112). We thank the development groups of ECHAM5, NEMO and OASIS for providing the component models and coupler, which are used under their respective licenses. We thank Jing-Jia LUO and Hui DING for helpful discussion. We also thank the two anonymous reviewers for their constructive advice.

REFERENCES

- Adler, R., and Coauthors, 2003: The version-2 global precipitation climatology project (GPCP) monthly precipitation analysis (1979–present). *Journal of Hydrometeorology*, **4**, 1147–1167.
- Brown, J. R., R. A. Colman, A. F. Moise, and I. N. Smith, 2013: The western Pacific monsoon in CMIP5 models: Model evaluation and projections. *J. Geophys. Res.*, **118**, doi: 10.1002/2013JD020290.
- Davey, M., and Coauthors, 2002: STOIC: A study of coupled model climatology and variability in tropical ocean regions. *Climate Dyn.*, **18**, 403–420.
- Deser, C., M. A. Alexander, S.-P. Xie, and A. S. Phillips, 2010: Sea surface temperature variability: Patterns and mechanisms. *Annual Review of Marine Science*, **2**, 115–143.
- Du, Z. C., R. H. Huang, and G. Huang, 2010: A weighting ensemble method by pattern correlation coefficients in sliding windows and its application to ensemble simulation and prediction of Asian summer monsoon precipitation by IPCC-AR4 multi-models. *Chinese J. Atmos. Sci.*, **34**, 1168–1186. (in Chinese).
- Fichefet, T., and M. A. M. Maqueda, 1997: Sensitivity of a global

- sea ice model to the treatment of ice thermodynamics and dynamics. *J. Geophys. Res.*, **102**, 12 609–12 646.
- Gualdi, S., A. Navarra, E. Guilyardi, and P. Delecluse, 2003: Assessment of the tropical Indo-Pacific climate in the SINTEX CGCM. *Annals of Geophysics*, **46**, doi: 10.4401/ag-3385.
- Guilyardi, E., 2006: El Niño-mean state-seasonal cycle interactions in a multi-model ensemble. *Climate Dyn.*, **26**, 329–348.
- Hu, K., G. Huang, X.-T. Zheng, S.-P. Xie, X. Qu, Y. Du, and L. Liu, 2014: Interdecadal variations in ENSO influences on Northwest Pacific-East Asian early summertime climate simulated in CMIP5 models. *J. Climate*, doi: 10.1175/JCLI-D-13-00268.1, in press.
- Huang, P., and R. Huang, 2009: Relationship between the modes of winter tropical Pacific SST anomalies and the intraseasonal variations of the following summer rainfall anomalies in China. *Atmos. and Oceanic Sci. Lett.*, **2**, 295–300.
- Huang, P., and R. Huang, 2010: Effects of the El Niño events on intraseasonal variations of following summer rainfall in China and its mechanism. *Transactions of Atmospheric Sciences*, **33**, 513–519. (in Chinese)
- Huang, R. H., 2006: Progress in the research on the formation mechanism and prediction theory of severe climatic disasters in China. *Adv. Earth Sci.*, **21**, 564–575. (in Chinese)
- Huang, R.-H., and W. Li, 1987: Influence of the heat source anomaly over the tropical western Pacific on the subtropical high over East Asia. *Proceedings of the International Conference on the General Circulation of East Asia*, Chengdu, 40–51.
- Huang, R. H., and Y. F. Wu, 1989: The influence of ENSO on the summer climate change in China and its mechanism. *Adv. Atmos. Sci.*, **6**, 21–33.
- Huang, R. H., W. Chen, B. Yang, and R. Zhang, 2004: Recent advances in studies of the interaction between the East Asian winter and summer monsoons and ENSO cycle. *Adv. Atmos. Sci.*, **21**, 407–424.
- Huang, R. H., J. Chen, and G. Huang, 2007: Characteristics and variations of the East Asian monsoon system and its impacts on climate disasters in China. *Adv. Atmos. Sci.*, **24**, 993–1023, doi: 10.1007/s00376-007-0993-x.
- Kalnay, E., and Coauthors, 1996: The NCEP/NCAR 40-year reanalysis project. *Bull. Amer. Meteor. Soc.*, **77**, 437–471.
- Kosaka, Y., and H. Nakamura, 2006: Structure and dynamics of the summertime Pacific-Japan teleconnection pattern. *Quart. J. Roy. Meteor. Soc.*, **132**, 2009–2030.
- Kosaka, Y., S.-P. Xie, N.-C. Lau, and G. A. Vecchi, 2013: Origin of seasonal predictability for summer climate over the northwestern Pacific. *Proc. Natl. Acad. Sci. USA*, **110**, 7574–7579.
- Latif, M., and Coauthors, 2001: ENSIP: The El Niño simulation intercomparison project. *Climate Dyn.*, **18**, 255–276.
- Li, G., and S.-P. Xie, 2014: Tropical biases in CMIP5 multi-model ensemble: The excessive equatorial Pacific cold tongue and double ITCZ problems. *J. Climate*, **27**, 1765–1780, doi: JCLI-D-13-00337.1.
- Luo, J.-J., S. Masson, E. Roeckner, G. Madec, and T. Yamagata, 2005: Reducing climatology bias in an ocean-atmosphere CGCM with improved coupling physics. *J. Climate*, **18**, 2344–2360.
- Ma, C.-C., C. R. Mechoso, A. W. Robertson, and A. Arakawa, 1996: Peruvian stratus clouds and the tropical Pacific circulation: A coupled ocean-atmosphere GCM study. *J. Climate*, **9**, 1635–1645.
- Madec, G., 2008: NEMO ocean engine. Note du Pole de modelisation 27, Institut Pierre-Simon Laplace, 193 pp.
- Mechoso, C. R., and Coauthors, 1995: The seasonal cycle over the tropical Pacific in coupled ocean-atmosphere general circulation models. *Mon. Wea. Rev.*, **123**, 2825–2838.
- Nitta, T., 1987: Convective activities in the tropical western Pacific and their impact on the Northern Hemisphere summer circulation. *J. Meteor. Soc. Japan*, **65**, 373–390.
- Park, W., N. Keenlyside, M. Latif, A. Ströh, R. Redler, E. Roeckner, and G. Madec, 2009: Tropical Pacific climate and its response to global warming in the Kiel climate model. *J. Climate*, **22**, 71–92.
- Rasmusson, E. M., and T. H. Carpenter, 1982: Variations in tropical sea surface temperature and surface wind fields associated with the Southern Oscillation/El Niño. *Mon. Wea. Rev.*, **110**, 354–384.
- Rayner, N., and Coauthors, 2003: Global analyses of sea surface temperature, sea ice, and night marine air temperature since the late nineteenth century. *J. Geophys. Res.*, **108**, 4407.
- Roeckner, E., and Coauthors, 2003: The atmospheric general circulation model ECHAM5. PART I: Model description. Report 349, Max Planck Institute for Meteorology, 140 pp.
- Roeckner, E., and Coauthors, 2006: Sensitivity of simulated climate to horizontal and vertical resolution in the ECHAM5 atmosphere model. *J. Climate*, **19**, 3771–3791.
- Song, F. F., and T. J. Zhou, 2014: Inter-annual variability of East Asian summer monsoon simulated by CMIP3 and CMIP5 AGCMs: Skill dependence on Indian Ocean-western Pacific anticyclone teleconnection. *J. Climate*, **27**, 1679–1697, doi: 10.1175/JCLI-D-13-00248.1.
- Sperber, K. R., and Coauthors, 2013: The Asian summer monsoon: An intercomparison of CMIP5 vs. CMIP3 simulations of the late 20th century. *Climate Dyn.*, **41**, 2711–2744.
- Valcke, S., 2006: OASIS3 user guide. PRISM Tech. Rep. 3, 64 pp.
- Wang, B. I. N., R. Wu, and T. I. M. Li, 2003: Atmosphere-warm ocean interaction and its impacts on Asian-Australian monsoon variation. *J. Climate*, **16**, 1195–1211.
- Wang, C., and J. Picaut, 2004: Understanding ENSO physics—A review. *Earth's Climate: The Ocean-Atmosphere Interaction*, C. Wang, S.-P. Xie, and J. Carton, Eds., AGU Geophysical Monograph Series, 21–48.
- Xie, S.-P., K. Hu, J. Hafner, H. Tokinaga, Y. Du, G. Huang, and T. Sampe, 2009: Indian Ocean capacitor effect on Indo-western Pacific climate during the summer following El Niño. *J. Climate*, **22**, 730–747.
- Zhang, R., A. Sumi, and M. Kimoto, 1996: Impact of El Niño on the East Asian monsoon: A diagnostic study of the '86/87 and '91/92 events. *J. Meteor. Soc. Japan*, **74**, 49–62.
- Zhang, R. H., A. Sumi, and M. Kimoto, 1999: A diagnostic study of the impact of El Niño on the precipitation in China. *Adv. Atmos. Sci.*, **16**, 229–241.
- Zheng, Y., J. L. Lin, and T. Shinoda, 2012: The equatorial Pacific cold tongue simulated by IPCC AR4 coupled GCMs: Upper ocean heat budget and feedback analysis. *J. Geophys. Res.*, **117**, C05024, doi: 10.1029/2011JC007746.